

Journal Pre-proof

Free volume manipulation of a 6FDA-HAB polyimide using a solid-state protection/deprotection strategy

Sharon Lin, Taigyu Joo, Francesco M. Benedetti, Laura C. Chen, Albert X. Wu, Katherine Mizrahi Rodriguez, Qihui Qian, Cara M. Doherty, Zachary P. Smith



PII: S0032-3861(20)30946-0

DOI: <https://doi.org/10.1016/j.polymer.2020.123121>

Reference: JPOL 123121

To appear in: *Polymer*

Received Date: 28 May 2020

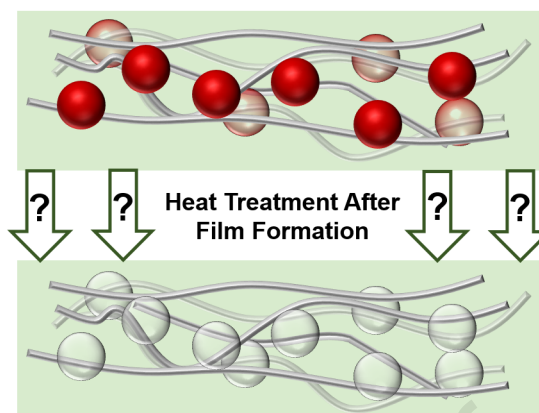
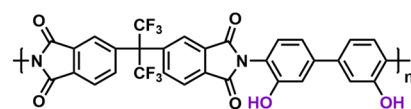
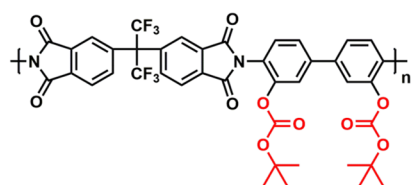
Revised Date: 15 August 2020

Accepted Date: 7 October 2020

Please cite this article as: Lin S, Joo T, Benedetti FM, Chen LC, Wu AX, Rodriguez KM, Qian Q, Doherty CM, Smith ZP, Free volume manipulation of a 6FDA-HAB polyimide using a solid-state protection/deprotection strategy, *Polymer*, <https://doi.org/10.1016/j.polymer.2020.123121>.

This is a PDF file of an article that has undergone enhancements after acceptance, such as the addition of a cover page and metadata, and formatting for readability, but it is not yet the definitive version of record. This version will undergo additional copyediting, typesetting and review before it is published in its final form, but we are providing this version to give early visibility of the article. Please note that, during the production process, errors may be discovered which could affect the content, and all legal disclaimers that apply to the journal pertain.

© 2020 Published by Elsevier Ltd.



Free volume manipulation of a 6FDA-HAB polyimide using a solid-state protection/deprotection strategy

Sharon Lin,^a Taigyu Joo,^a Francesco M. Benedetti,^a Laura C. Chen,^a Albert X. Wu,^a Katherine Mizrahi Rodriguez,^b Qihui Qian,^a Cara M. Doherty,^c and Zachary P. Smith^{a,*}

^a Department of Chemical Engineering, Massachusetts Institute of Technology, Cambridge, MA 02139, United States

^b Department of Materials Science and Engineering, Massachusetts Institute of Technology, Cambridge, MA 02139, United States

^c The Commonwealth Scientific and Industrial Research Organization (CSIRO) Manufacturing, Private Bag 10, Clayton South 3169, Victoria, Australia

* Corresponding Author. Email address: zpsmith@mit.edu; Postal address: Massachusetts Institute of Technology, Department of Chemical Engineering, 77 Massachusetts Avenue, Room 66-466, Cambridge, MA, USA 02139-4307

ABSTRACT

Tert-butoxycarbonyl (t-BOC) is a thermally labile moiety that can be used to protect hydroxyl groups on polymers. In this study, t-BOC was appended onto a polyimide consisting of 2,2'-bis-(3,4-dicarboxyphenyl) hexafluoropropane dianhydride (6FDA) and 3,3'-dihydroxy-4,4'-diamino-biphenyl (HAB), after which the polymer was formed into self-standing films. Solid-state thermal treatments were performed to systematically remove t-BOC moieties to alter the physical packing structure and concomitant gas transport properties of the polymer. Despite performing deprotection reactions well below the glass transition temperature of 6FDA-HAB (~300 °C), this free volume manipulation (FVM) approach produced only subtle differences in polymer density, fractional free volume, average free volume element size, and gas transport properties relative to the unprotected polymer. While these findings suggest that thermally removing covalently bound functional groups from polymer films can be used to manipulate free volume and gas transport performance for glassy polymers, more robust polymer systems than linear polyimides are required to preserve the nascent free volume architecture generated from this approach.

KEYWORDS

Thermal modification, gas transport, polyimide films, free volume modification

1. Introduction

Polymer membranes have shown great promise for applications in energy-efficient gas separations, such as nitrogen enrichment, oxygen generation, and natural gas sweetening [1–3]. In order to be suitable for gas separations, membrane materials should be solution-processable, highly permeable, and selective [1]. A general strategy to improve permeability is to generate high free volume materials, and along these lines, “bottom up” approaches such as synthesizing rigid and contorted backbones have resulted in impressive advancements in materials performance [4]. Most notably, polymers of intrinsic microporosity (PIMs) have continued to surpass upper bound performance limits by incorporating bulky groups into the polymer backbone such as Tröger’s base and triptycene [4–10]. Thermally rearranged (TR) polymers have also been used to tune free volume size and distribution [11–13]. An alternative strategy, however, is to use a “top down” approach to modify free volume from thermal decomposition of functional groups in the solid state.

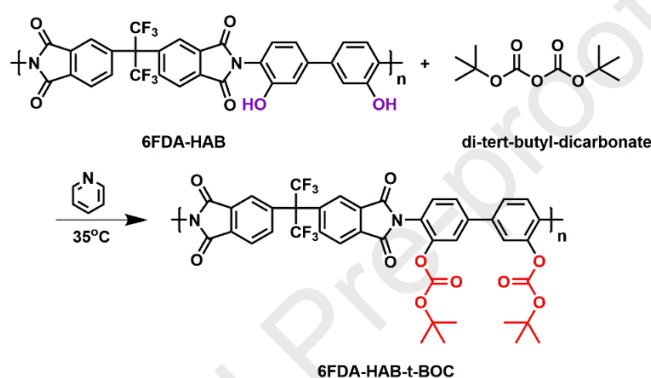
In the 1980s and 1990s, researchers in the field of lithography began to investigate high glass transition temperature materials such as polyimides [14]. Of note, Omote et al. demonstrated that a polyimide (6FDA-AHHFP) that contained hydroxyl functional groups could be functionalized with tert-butoxycarbonyl (t-BOC), cast into a film, and then thermally- or UV-treated in the presence of an acid to remove t-BOC [15]. A more recent study by Fukumaru et al. demonstrated that thermally removing t-BOC groups from functionalized films of poly(p-phenylene benzobisoxazole) (PPBO) could generate porosity [16]. Merlet et al. also showed that the thermal removal of t-BOC from a poly(phenylquinoxaline) (PPQ) backbone could lead to the generation of free volume elements in the polymer matrix [17,18]. In the field of gas separations, Chung and coworkers have used this approach to generate free volume elements by thermally

treating polyimide films to remove labile functional groups such as cyclodextrine [19–21] or various saccharides [22]. Zhou et al. and Islam et al. both reported increases in permeability after thermally removing sulfonic acid groups from a polyimide at temperatures above the glass transition temperature of the polymer [23,24]. Maya et al. investigated in situ pyrolysis and thermal crosslinking of carboxylic acid functionality on a polyimide that led to changes in free volume distribution [25]. In addition, Martínez-Mercado et al. reported that short thermal treatments (i.e. < 3.5 h) at moderate temperatures (160–180 °C) of a poly(oxindole biphenylene) film with a –CH₂OH group led to higher gas permeabilities [26]. There are also indications of applying this “top down” approach in the patent literature [27].

While the aforementioned studies indicate some success in post-synthetically generating free volume using thermal treatments, other studies report a decrease in free volume. In a study by Sánchez-García et al., it was found that thermally removing t-BOC from poly(oxindole biphenylene) resulted in decreases in fractional free volume (FFV) and permeability, but an increase in selectivity [28]. Similar results were reported by Hernández-Martínez et al. [29]. Notably, thermal treatment can accelerate densification of glassy polymer films, which leads to decreased FFV and permeability [30–35]. Therefore, a systematic study is needed to evaluate the role of deprotection in the glassy state and concomitant changes in morphology and transport without competing effects such as cross-linking, which are common features of other studies [19–23,25,27,29].

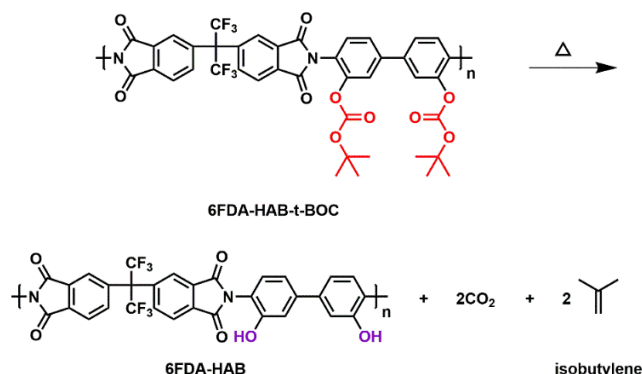
In this study, we seek to extend the “top down” approach of free volume manipulation (FVM) to further understand the effects of thermal treatment on gas transport properties of glassy polymers with thermally labile functional groups. The model polymer selected for this study is a 6FDA (2,2'-bis-(3,4-dicarboxyphenyl) hexafluoropropane dianhydride)-based polyimide because

these polymers have been studied as promising membrane materials for many years [36–39]. More specifically, we investigated 6FDA-HAB [40–43], which combines 6FDA with a diamine, HAB (3,3'-dihydroxy-4,4'-diamino-biphenyl), that contains hydroxyl groups that can react with di-tert-butyl-dicarbonate to generate a BOC-protected polyimide. BOC protection of 6FDA-HAB, as shown in **Scheme 1**, results in a polyimide that will henceforth be referred to as “6FDA-HAB-t-BOC”.



Scheme 1: BOC protection of 6FDA-HAB. The ortho-positioned functional groups are shown in purple for 6FDA-HAB and in red for 6FDA-HAB-t-BOC.

After being cast into a film, 6FDA-HAB-t-BOC can be thermally treated to deprotect the t-BOC group, as presented in **Scheme 2**. The thermal decomposition of t-BOC results in two gaseous products, CO₂ and isobutylene [15,28]. In this way, the original 6FDA-HAB chemical structure is recovered, but what remains is a polymer in an altered morphological state. By deprotecting 6FDA-HAB-t-BOC films using different treatment temperatures and times, this study seeks to systematically investigate the effects of treatment conditions on the free volume architecture of a linear polyimide.



Scheme 2: BOC deprotection of 6FDA-HAB-t-BOC.

2. Experimental

2.1. Materials

The aromatic dianhydride, 2,2'-bis-(3,4-dicarboxyphenyl) hexafluoropropane dianhydride (6FDA, 99.86%), was purchased from *Chem-Impex International, Inc.* and underwent vacuum sublimation at 235 °C for approximately 1 h before use. The diamine, 3,3'-dihydroxy-4,4'-diamino-biphenyl (HAB, >99.0%), was purchased from *TCI Chemicals* and dried under vacuum at 60 °C overnight before use. Di-tert-butyl-dicarbonate ($\geq 99\%$) was purchased from *Sigma-Aldrich* and used as received. Anhydrous 1-methyl-2-pyrrolidinone (NMP, 99.5%), anhydrous o-dichlorobenzene (o-DCB, 99%), methanol ($\geq 99.9\%$), pyridine (99.9%), dimethylacetamide (DMAc, $\geq 99.5\%$), N,N-dimethylformamide ($\geq 99.9\%$), and n-heptane ($\geq 96\%$) were obtained from *Sigma-Aldrich* and used as received. Chloroform ($\geq 99.8\%$) was purchased from *Macron Fine Chemicals* and used as received. Deuterated dimethyl sulfoxide (DMSO- d_6 , 99.9%) was purchased from *Cambridge Isotope Laboratories, Inc.* and used as received.

2.2. Synthesis of 6FDA-HAB polyimide and BOC protection

A three-neck flask fitted with an overhead mechanical stirrer was purged with nitrogen (*Airgas*, 99.999%) for 30 min to remove water vapor. HAB (8.008 mmol) and 30 mL of anhydrous NMP were added to the flask and stirred to dissolution. An equimolar amount of 6FDA (8.008 mmol) and an additional 20 mL of anhydrous NMP were added to the flask to generate a ~10.6 w/v% solution. The solution was then left stirring overnight, forming a viscous poly(amic acid).

Thermal imidization in solution was used to form a polyimide from the poly(amic acid). In this procedure, 12.5 mL of *o*-DCB was added to the reaction flask to form an ~8.5 w/v% solution. A reverse Dean-Stark trap with an overhead air condenser was then used to assist in the removal of water vapor with *o*-DCB acting as an azeotropic agent. The solution was heated to 180 °C for 24 h to convert the poly(amic acid) to a polyimide.

After imidization, the polymer was precipitated from the reaction solution using methanol that was stirring in a blender to produce a light brown and fibrous precipitate. In order to extract solvent, the precipitated 6FDA-HAB polyimide was filtered and rinsed with methanol before stirring in fresh methanol for an additional 24 h. The polyimide was filtered again, rinsed with fresh methanol for a second time, and stirred in fresh methanol for another 24 h. This solvent extraction procedure was performed one additional time. The polyimide was then placed on a glass dish and dried under full vacuum at 200 °C and 225 °C for 24 h and 48 h, respectively.

To generate 6FDA-HAB-t-BOC, an equimolar amount of pyridine (which acted as a catalyst for BOC protection) and di-*tert*-butyl-dicarbonate (24.025 mmol) was added directly to the reaction solution after imidization. The reaction was allowed to proceed for 24 h at 35 °C. The polymer was then precipitated (as a light tan precipitate) and washed in an identical fashion

to that of 6FDA-HAB. After the last methanol wash, 6FDA-HAB-t-BOC was placed on a glass dish and left to dry at room temperature in a chemical fumehood for 48 h.

2.3. Film fabrication and thermal treatment of 6FDA-HAB-t-BOC films

6FDA-HAB was dissolved in DMAc (1 w/v%) for 24 h at 90 °C, similar to a previously reported procedure [12]. The solution was then filtered through a 5 µm Whatman PTFE syringe filter (*GE Healthcare Life Sciences*) onto a 5 cm diameter flat-bottomed glass dish and heated at 60 °C for 48 h under –10 inHg (–34 kPa) vacuum, following a similarly reported procedure [12]. During this process, vaporized solvent from the headspace of the vacuum oven was occasionally removed by pulling vacuum while opening the vacuum pump vent to maintain an oven pressure of –10 inHg (–34 kPa). Solvent was collected using a solvent trap submerged in liquid nitrogen. The formed films were then exposed to full vacuum for 1 h and then heated at 200 °C and 225 °C for 24 h and 48 h, respectively, to remove residual solvent. The 6FDA-HAB films, which were 10–15 µm in thickness, were removed from the glass dish by submersion in deionized water for 10 min.

Since the boiling point of DMAc is 165 °C, which is above the reported BOC deprotection temperature of 150 °C, a solvent with a lower boiling point of 61 °C, chloroform (3 w/v%), was required to cast 6FDA-HAB-t-BOC so that the solvent could subsequently be removed without BOC deprotection. It should be noted that 6FDA-HAB was found to be insoluble in solvents with boiling points lower than that of DMAc. The 6FDA-HAB-t-BOC solution was filtered through a 0.45 µm PTFE syringe filter (*VWR*, 28145-497) onto a 5 cm diameter flat-bottomed glass dish. The glass dish was covered with aluminum foil and another glass dish as a cover, thereby enabling film formation via slow solvent evaporation inside a

chemical fumehood for 72 h. The films, which were 10–35 μm in thickness, were removed from the glass dish by submersion in deionized water for 10 min, and the film was heated at 90 $^{\circ}\text{C}$ under full vacuum for 16 h to remove residual solvent.

Three treatment temperatures were selected to study the effects of temperature on BOC deprotection and the resulting polymer properties. 6FDA-HAB-t-BOC films were held at 130 $^{\circ}\text{C}$, 140 $^{\circ}\text{C}$, or 160 $^{\circ}\text{C}$ using a forced air convection oven with a temperature accuracy of ± 1 $^{\circ}\text{C}$ (*Lab Safety Supply*, #32EZ25). Since 130 $^{\circ}\text{C}$ and 140 $^{\circ}\text{C}$ are both below the prominent deprotection temperature of t-BOC, these experiments allowed for slower deprotection. The hold times considered at both of these temperatures were identical. However, because 160 $^{\circ}\text{C}$ is above the prominent deprotection temperature of t-BOC, hold times considered for this temperature were shorter. The oven was pre-heated to the designated temperature before placing a 6FDA-HAB-t-BOC film onto a flat glass dish inside the oven. Thermal treatment protocols are shown in **Table 1**, and samples are thus named according to their treatment protocol (i.e., samples treated at 130 $^{\circ}\text{C}$ for 1 h are labeled as “t-BOC-130-1h”).

Table 1: Thermal treatment protocols for 6FDA-HAB-t-BOC films.

Temperature ($^{\circ}\text{C}$)	Hold times
130	1 h, 2 h, 16 h
140	1 h, 2 h, 16 h
160	5 min, 15 min, 16 h

2.4. Characterization

^1H nuclear magnetic resonance (NMR) spectroscopy was performed using a *Bruker Avance Neo402* spectrometer to confirm the chemical structures of all samples in this study. 6FDA-HAB and 6FDA-HAB-t-BOC, in their powder form, as well as 6FDA-HAB-t-BOC and

thermally-treated 6FDA-HAB-t-BOC films, were dissolved in DMSO-d₆ (10 w/v%). Percent conversion (%) for each sample undergoing thermal treatment was determined by comparing relative peak integrations of BOC to hydroxyl functional groups. Percent conversion and the corresponding uncertainty are reported as the average and standard deviation, respectively, of at least 3 measurements. Heteronuclear single quantum correlation (HSQC) was run on a *Bruker Avance Neo500* spectrometer for t-BOC-130-1h dissolved in DMSO-d₆ (10 w/v%) to confirm the presence of isobutylene. A ¹H NMR spectrum of a solution of DMSO-d₆ and dosed-in isobutylene gas (*Airgas*, ≥ 99%) was also collected to further confirm isobutylene presence.

The molecular weight of 6FDA-HAB was determined using a *Waters* gel permeation chromatograph with a polystyrene (PS) reference and a mobile phase of DMF with 0.01 M lithium bromide. Chloroform GPC was performed on 6FDA-HAB-t-BOC using a *Tosoh EcoSEC HLC-8320* gel permeation chromatograph with *Dual TSKgel SuperH3000* columns, a PS reference, and a mobile phase of chloroform with 0.75% ethanol preservative.

Thermogravimetric analysis (TGA) was performed on all samples using a *TA Instruments TGA550*. Samples were heated from room temperature at a rate of 10 °C/min up to 800 °C in a nitrogen atmosphere. Nitrogen gas was flushed at a flow rate of 20 mL/min over the TGA balance and 40 mL/min in the sample chamber. TGA scans for 6FDA-HAB and thermally treated samples were normalized by their weight percent at 100 °C to eliminate the mass loss of atmospheric moisture that can strongly associate with polar groups in the polyimides.

The glass transition temperature (*T_g*) of 6FDA-HAB and 6FDA-HAB-t-BOC films was measured using a *TA Instruments DSC250* differential scanning calorimeter (DSC). Samples were heated at 10 °C/min from 25 °C to 350 °C under a nitrogen atmosphere with a flowrate of

50 mL/min. Three scans were taken for each sample, and the T_g was taken as the midpoint in the step change in heat capacity of the third scan.

Fourier transform infrared spectroscopy (FTIR) in attenuated total reflection (ATR) mode was performed using a *Bruker ALPHA FT-IR Spectrometer*. The spectra have a resolution of 4 cm^{-1} , and 256 scans per sample were performed in the range of 400–4000 cm^{-1} .

Density was measured using a *Mettler Toledo* density measurement kit (*ME-DNY-4*). Because of its slow uptake in polyimide samples, n-heptane was used as the buoyant liquid [43]. The density and corresponding uncertainty for each sample were taken as the average and standard deviation, respectively, of at least 3 measurements.

Positron annihilation lifetime spectroscopy (PALS) was performed on an automated *EG&G ORTEC* fast-fast coincidence system under vacuum at room temperature. During a PALS experiment, positrons from a radioisotope source enter the material and will either annihilate in the presence of free electrons or form a positronium (Ps) atom [44]. The Ps atom can exist either as a parapositronium (pPs) or an orthopositronium (oPs) atom [44]. Since Ps atoms can only form in areas of low electron density such as within the free volume elements of amorphous polymers [45–48], PALS can be used to determine the average free volume element size from correlations with the oPs lifetime. To conduct a PALS experiment, a Mylar envelope containing a ^{22}Na radioisotope source was placed in between two stacks of polymer films, and the envelope-film stack was wrapped in aluminum foil. At least 5 files of 4.5×10^6 integrated counts per file were collected for each sample, and data was analyzed with a three-component model using LT9 [49]. The three components consisted of the pPs atom, the free positron, and the oPs atom [44]. The lifetime of the pPs atom was fixed at $\tau_1 = 0.125$ ns [50], while the lifetimes of the free positron ($\tau_2 \sim 0.4$ ns) and oPs atom (τ_3), as well as the intensities (I) of all three components,

were fit using least squares optimization by the LT9 program. The error for τ_3 for each sample was taken as the standard deviation of the τ_3 values calculated from each file. The average size of free volume elements was calculated using a spherical assumption for free volume shape and the Tao-Eldrup equation [50,51]:

$$\tau_3 = \frac{1}{2} \left[1 - \frac{R}{R_0} + \frac{1}{2\pi} \sin \left(\frac{2\pi R}{R_0} \right) \right]^{-1} \quad (1)$$

in which R is the radius of the free volume element, ΔR is an empirical parameter determined to be 1.66 Å, and $R_0 = R + \Delta R$ [44,52]. Since low intensities were found for some samples, which may indicate oPs inhibition from the polar hydroxyl functionality [50,53], we do not report calculated free volume size distributions.

2.5. Pure-gas permeability measurements

Pure-gas permeabilities were evaluated at ~1 bar (100 kPa) for He, H₂, CH₄, N₂, O₂, and CO₂ at 35 °C for each sample using an automated constant-volume, variable-pressure system from *Maxwell Robotics*. All gases were ultra-high purity and purchased from *Airgas*. Cut films of approximately 1 cm² were placed on top of a hole in the center of a circular brass disk and secured using epoxy (*Devcon 5 min Epoxy*), which was left to cure for at least 30 min. The samples were then sealed in a stainless steel permeation cell (*Millipore*), which was immersed in a water bath that was temperature controlled by an immersion circulator (*ThermoFisher SC150L*). Before testing permeation, the testing chamber was dosed with ~2 bar (200 kPa) of helium gas to remove dissolved atmospheric gases. The sample was then held under vacuum at 35 °C for 8 h. Before switching to a new permeating gas, samples were again dosed with ~2 bar of helium and held under vacuum for at least six time lag-equivalents. Each sample was tested at least twice to confirm reproducibility.

Pure-gas permeability (P) was calculated using the following equation:

$$P = \frac{V_d l}{p_2 A R T} \left[\left(\frac{dp}{dt} \right)_{ss} - \left(\frac{dp}{dt} \right)_{leak} \right] \quad (2)$$

where V_d is the downstream volume, l is the film thickness, p_2 is the upstream pressure, A is the area of film exposed to the gas, R is the ideal gas constant, T is the absolute experimental temperature, $\left(\frac{dp}{dt} \right)_{ss}$ is the rate of pressure rise in the permeate at steady state, and $\left(\frac{dp}{dt} \right)_{leak}$ is the leak rate [54]. The ideal gas selectivity ($\alpha_{i,j}$) was taken to be the ratio of the pure-gas permeabilities of the more permeable gas, i , to that of the less permeable gas, j (i.e., $\frac{P_i}{P_j}$). Diffusion coefficients for each gas were determined using the time-lag method, $D = \frac{l^2}{6\theta}$, in which θ is the time lag [55]. Sorption coefficients were calculated using the sorption–diffusion model ($S = \frac{P}{D}$) [56]. Error bars for permeability, diffusion coefficients, and sorption coefficients were determined by error propagation [57]. Time-lag values obtained for He and H₂ were within the resolution of acquisition time (i.e., 1–2 s) of the permeation systems, and thus could not be accurately determined. We therefore only include diffusion and sorption coefficients calculated from the time-lag method for N₂, O₂, CH₄, and CO₂, which all yielded time-lags greater than 6.2 s, which is significantly longer than the acquisition time of the permeation system.

3. Results and Discussion

3.1. Characterization of 6FDA-HAB polyimide and BOC-protection

Fully assigned ¹H NMR spectra of both 6FDA-HAB and 6FDA-HAB-t-BOC powder samples are reported in Section S1. In the ¹H NMR spectrum of 6FDA-HAB-t-BOC, there is a singlet at 1.25 ppm, which corresponds to the protons in the t-BOC functional group. The

presence of this singlet and the absence of a hydroxyl proton singlet at 10.08 ppm indicate successful BOC protection. GPC analysis indicated that BOC protection had a minimal impact on molecular weight (Section S1).

TGA scans of 6FDA-HAB and 6FDA-HAB-t-BOC powder are shown in **Figure 1**. In the TGA scan of 6FDA-HAB, two distinct regions of mass loss are clearly observed. The first region, which begins at approximately 400 °C, is attributed to thermal rearrangement of the polyimide (labeled as “TR” in **Figure 1**), while the second region, which begins at approximately 500 °C, is attributed to thermal degradation [11,12]. The process of thermal rearrangement, a decarboxylation process, leads to structural changes in polyimides that contain ortho-positioned functional groups, such as 6FDA-HAB [11]. In the TGA scan of 6FDA-HAB-t-BOC, a third distinct region of mass loss is clearly observed starting at approximately 150 °C. This mass loss, which was determined to be 25.9 wt%, is associated with the removal of t-BOC from the polymer backbone [15,28,29]. This finding correlates well with the theoretical weight percent of t-BOC on the polymer backbone, which is 24.8 wt%. The stable sample weight across a broad temperature range between BOC deprotection and the TR region of the polyimide indicates that these two processes occur independently, which makes this system ideal for exclusively studying the effects of t-BOC removal without competing chemical reactions.

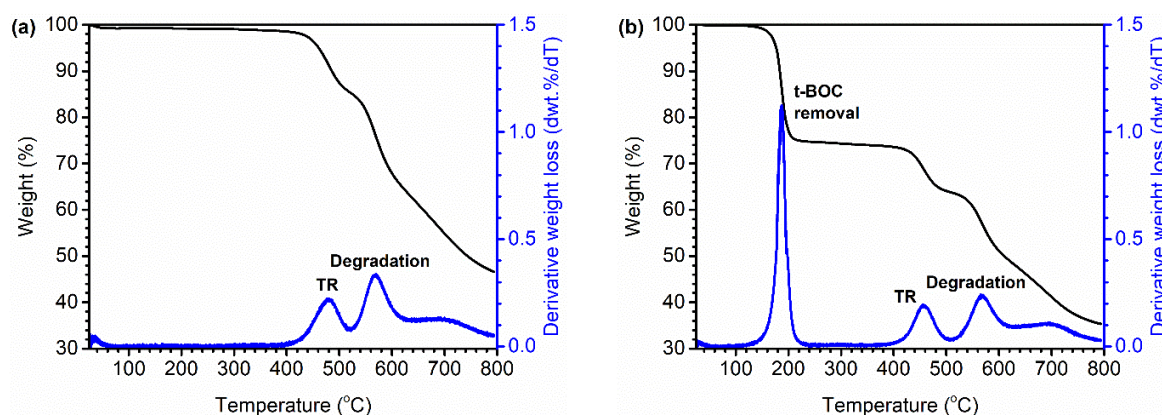


Figure 1: TGA scans of (a) 6FDA-HAB and (b) 6FDA-HAB-t-BOC powder. Distinct regions of mass loss are labeled accordingly.

From DSC, the T_g of 6FDA-HAB was found to be approximately 300 °C, while the T_g of the deprotected 6FDA-HAB-t-BOC sample was approximately 306 °C (Section S1). Given the rather broad temperature range for these transitions, the T_g values between the two samples are roughly equivalent. Guo et al. previously reported differences in T_g for acetate-functionalized variants 6FDA-HAB [42], but acetate moieties are more thermally stable than t-BOC, and hence, are not removed below the polymer T_g . Thus, for our work, similar values of T_g for 6FDA-HAB and the deprotected 6FDA-HAB-t-BOC are expected because both samples have an identical chemical structure.

3.2. Thermal treatment of 6FDA-HAB-t-BOC films

Optically transparent films of 6FDA-HAB, 6FDA-HAB-t-BOC, and thermally treated 6FDA-HAB-t-BOC are presented in Section S1. Upon heating, the optically clear 6FDA-HAB-t-BOC turns slightly yellow, indicating a shift in color that more closely matches that of 6FDA-HAB. FTIR measurements also indicated that thermal treatments resulted in the conversion of 6FDA-HAB-t-BOC to 6FDA-HAB (Section S1).

^1H NMR was used to track the extent of deprotection for each thermal treatment condition, as shown in **Figure 2**. Spectra for 6FDA-HAB and 6FDA-HAB-t-BOC are included for reference. It is important to note that the 6FDA-HAB-t-BOC spectrum was obtained from films that had previously been heated at 90 °C under full vacuum to remove solvent. All ^1H NMR spectra shown in **Figure 2** were normalized by the proton in the polymer backbone labeled “B” in Figure S1. The ratios of peak integrations were used to determine the percent conversion

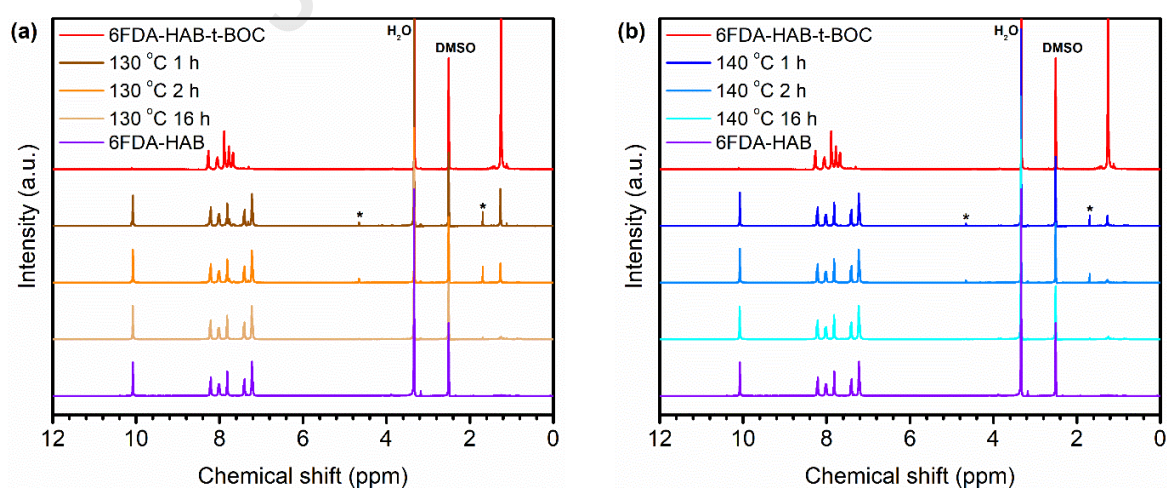
of 6FDA-HAB-t-BOC to 6FDA-HAB, and these results are tabulated in **Table 2**. From this analysis, we can confirm that film formation and solvent removal for 6FDA-HAB-t-BOC resulted in minimal deprotection, as a small peak at 10.08 ppm can be seen in the ^1H NMR spectrum of the 6FDA-HAB-t-BOC film, indicating approximately $4\% \pm 0.5\%$ hydroxyl functionality. The concomitant decrease in the t-BOC proton singlet peak at 1.25 ppm and the increase in the hydroxyl proton singlet peak at 10.08 ppm indicate that more t-BOC was removed with increasing time at a set temperature. As expected, for 1 or 2 h hold times, thermal treatments at 140 °C removed similar or more t-BOC than thermal treatments at 130 °C. For thermal treatments of 16 h, conversion was always approximately 95%, regardless of temperature, indicating a conversion limit for these samples.

Two additional peaks were occasionally observed in NMR spectra at 1.69 ppm and 4.66 ppm, which are associated with isobutylene. While the thermal decomposition products of t-BOC are CO_2 and isobutylene, the timescales of diffusion for these two molecules are vastly different. Time-lag experiments, which will be presented later, suggest that CO_2 diffuses completely from the film during thermal treatment, while these ^1H NMR results show the presence of some isobutylene after deprotection. HSQC spectroscopy was performed on t-BOC-130-1h to confirm the presence of isobutylene (Section S2). ^1H NMR was also performed on a solution of isobutylene gas dosed in DMSO-d_6 to further confirm the presence of isobutylene in thermally treated samples (Section S2). Interestingly, the intensities of the isobutylene peaks decrease at longer conversion times and become negligible after 16 h treatments at each temperature because enough time was provided for isobutylene molecules to diffuse out of the film. An estimation of isobutylene content (Section S3) revealed that only trace amounts of isobutylene remained in some samples prior to characterization. Within the uncertainty of our analysis procedure ($\pm 1\%$),

no detectable isobutylene remained in six of our nine thermally treated samples prior to permeation testing. For the three samples with detectable isobutylene content, the highest content was about 3 wt% for t-BOC-160-5min. Therefore, experiments were run without further treatment to avoid complications that could result from physical aging and thermal annealing.

Table 2: Percent conversion of 6FDA-HAB-t-BOC films that underwent thermal treatment, as determined from ^1H NMR.

Treatment Temperature ($^{\circ}\text{C}$)	Hold time	Percent conversion (%)
130	1 h	88.5 ± 0.5
	2 h	93 ± 1
	16 h	95.7 ± 0.9
140	1 h	93 ± 1
	2 h	95 ± 1
	16 h	95.5 ± 0.1
160	5 min	87 ± 2
	15 min	95.0 ± 0.5
	16 h	94 ± 1



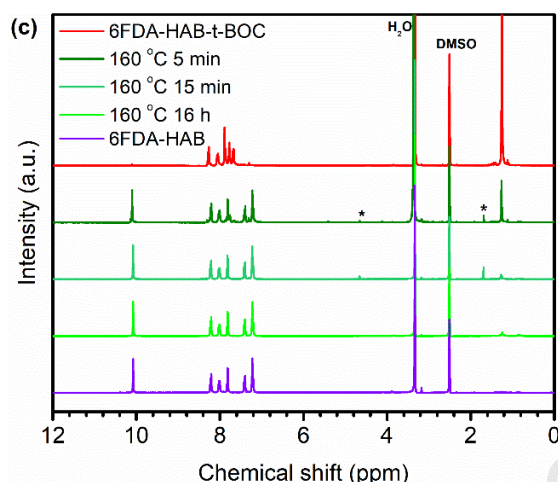


Figure 2: ^1H NMR spectra for 6FDA-HAB-t-BOC films undergoing thermal treatments at (a) 130 $^{\circ}\text{C}$, (b) 140 $^{\circ}\text{C}$, and (c) 160 $^{\circ}\text{C}$. Peaks that are labeled with a “*” are associated with the protons in isobutylene. ^1H NMR spectra of 6FDA-HAB and 6FDA-HAB-t-BOC are added for reference.

TGA scans for all films are shown in **Figure 3**. For all treatment temperatures, longer treatment times led to more t-BOC being removed from the polymer backbone, which is evident in the smaller decrease in weight percentage starting at 150 $^{\circ}\text{C}$. In contrast to the TGA profile for the 6FDA-HAB-t-BOC powder shown in **Figure 1**, TGA scans for the 6FDA-HAB-t-BOC films showed a gradual mass loss over extended temperature ranges well beyond 150 $^{\circ}\text{C}$. This finding suggests that the higher accessible surface area of the powders reduces the time required for diffusion of gaseous byproducts. While CO_2 is a smaller gas and thus can diffuse more readily, isobutylene is significantly larger and will diffuse more slowly. Therefore, the slow decrease in weight percent as the sample is heated after t-BOC removal until the beginning of thermal rearrangement at approximately 400 $^{\circ}\text{C}$ can be predominantly attributed to slow diffusion of isobutylene. This slow decrease in weight percent is present in all thermally treated samples, and

for this reason, it is challenging to accurately quantify the exact amount of t-BOC remaining on the polymer backbone using only TGA.

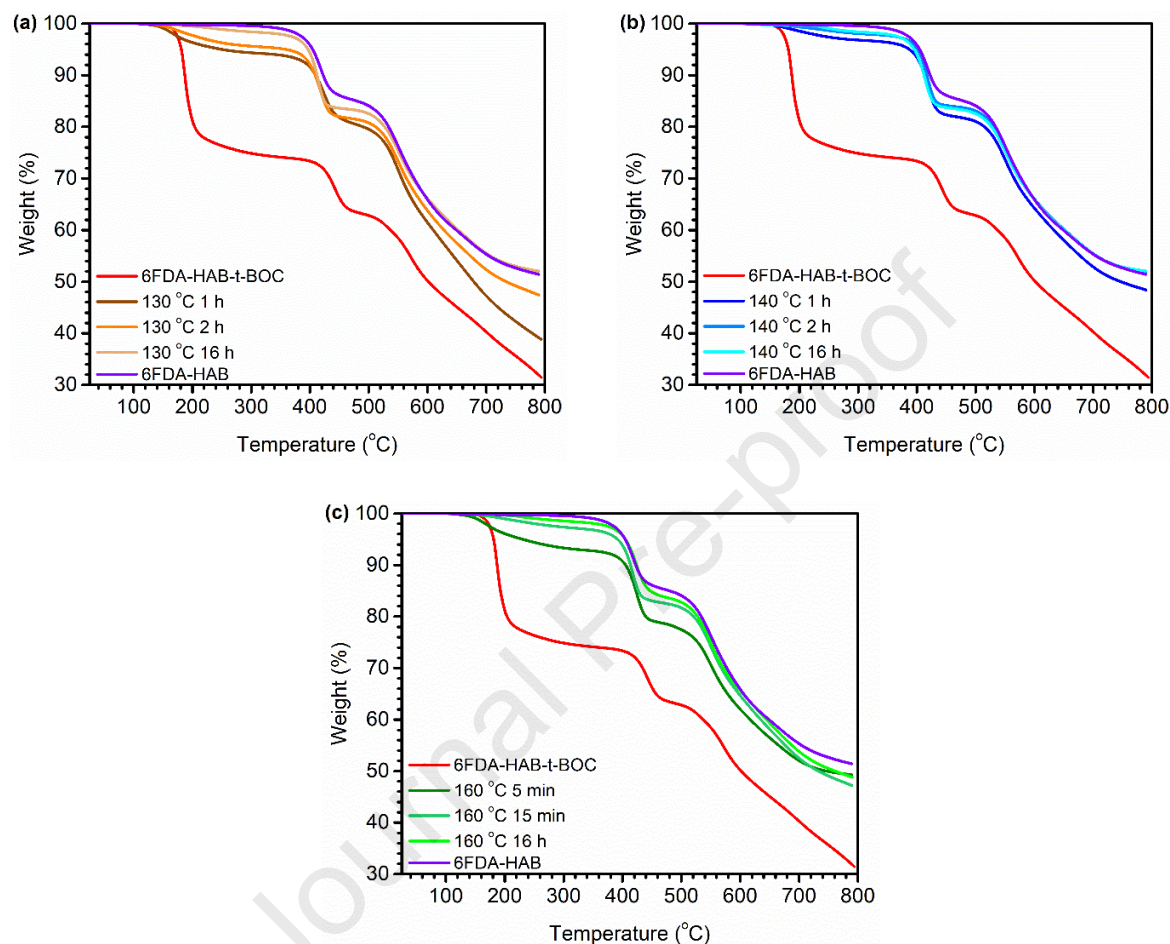


Figure 3: TGA scans for 6FDA-HAB and 6FDA-HAB-t-BOC reference samples, and 6FDA-HAB-t-BOC films that had previously undergone thermal treatments at (a) 130 °C, (b) 140 °C, and (c) 160 °C.

3.3. Effect of sample treatment on polymer chain packing

Fractional free volume (FFV) was calculated using the following equation:

$$FFV = \frac{V - 1.3V_w}{V} \quad (3)$$

where V is the molar volume of the polymer, and V_w is the van der Waals volume of the polymer determined using the group contribution method originally developed by Bondi [58–60]. For thermally treated 6FDA-HAB-t-BOC samples, van der Waals volumes were estimated as the molar arithmetic sum of t-BOC and hydroxyl structural units that remained on each sample:

$$V_w = x_1 V_{w1} + x_2 V_{w2} \quad (4)$$

in which x_1 and x_2 are mole fractions and V_{w1} and V_{w2} are van der Waals volumes (1: 6FDA-HAB-t-BOC, 2: 6FDA-HAB), essentially treating the thermally-treated samples as a co-polymer [61]. The calculated FFV, oPs lifetimes (τ_3) and intensities (I_3), and average free volume element radii (R) calculated from the Tao-Eldrup equation are presented in **Table 3**.

Table 3: Density, fractional free volume (FFV), PALS results (τ_3 and I_3), and average free volume element radius (R) for 6FDA-HAB, 6FDA-HAB-t-BOC, and 6FDA-HAB-t-BOC after various thermal treatments.

Sample	Treatment Temperature (°C)	Hold time	Density (g/cm ³)	FFV	τ_3 (ns)	I_3 (%)	R (Å)
6FDA-HAB	n/a	n/a	1.50 ± 0.04	0.11 ± 0.03	2.35 ± 0.04	2.0 ± 0.1	3.15 ± 0.03
6FDA-HAB-t-BOC	n/a	n/a	1.32 ± 0.02	0.18 ± 0.01	2.74 ± 0.02	9.82 ± 0.07	3.45 ± 0.01
6FDA-HAB-t-BOC	130	1 h	1.39 ± 0.02	0.17 ± 0.01	2.68 ± 0.03	8.53 ± 0.08	3.41 ± 0.02
		2 h	1.39 ± 0.02	0.17 ± 0.01	2.66 ± 0.02	7.08 ± 0.05	3.38 ± 0.02
		16 h	1.48 ± 0.05	0.12 ± 0.03	2.89 ± 0.05	3.04 ± 0.05	3.54 ± 0.03
6FDA-HAB-t-BOC	140	1 h	1.50 ± 0.02	0.11 ± 0.01	2.63 ± 0.03	6.72 ± 0.07	3.37 ± 0.02
		2 h	1.49 ± 0.05	0.12 ± 0.03	2.62 ± 0.02	5.17 ± 0.05	3.36 ± 0.01
		16 h	1.47 ± 0.05	0.13 ± 0.03	2.75 ± 0.05	2.59 ± 0.07	3.46 ± 0.04
6FDA-HAB-t-BOC	160	5 min	1.42 ± 0.02	0.15 ± 0.01	2.56 ± 0.01	8.06 ± 0.08	3.32 ± 0.01
		15 min	1.515 ± 0.003	0.101 ± 0.002	2.53 ± 0.04	6.7 ± 0.1	3.29 ± 0.03
		16 h	1.54 ± 0.04	0.09 ± 0.02	2.71 ± 0.05	3.6 ± 0.1	3.43 ± 0.04

Graphical comparisons of percent conversion from 6FDA-HAB-t-BOC to 6FDA-HAB versus FFV are depicted in **Figure 4a**. There is a significant amount of scatter in this plot, indicating a poor correlation between FFV and percent conversion, but a few salient observations can be made. As expected, the FFV of 6FDA-HAB-t-BOC is higher than that of 6FDA-HAB due

to the incorporation of t-BOC functional groups onto the polymer backbone. The bulkiness of this group is expected to reduce the efficiency of polymer chain packing in the film state, and the elimination of hydrogen bonding after protection of hydroxyl functional groups would likewise be expected to decrease polymer–polymer interactions. Similar observations between functionalized and non-functionalized polymer films have been reported in other studies [28,43,62]. For example, in a study by Sanders et al., larger ortho-positioned groups appended to 6FDA-HAB led to disrupted chain packing, lower density, and higher FFV values [43]. A hydroxyl functional 6FDA-HAB sample had an FFV value of $13\% \pm 1\%$, but upon functionalization with acetate, propanoate, or pivalate, FFV increased to $14.6\% \pm 0.5\%$, $15.0\% \pm 0.7\%$, and $18.1\% \pm 0.8\%$, respectively [43]. We observed similar trends, including an FFV value of $18\% \pm 1\%$ for 6FDA-HAB-t-BOC and $11\% \pm 3\%$ for 6FDA-HAB.

A weak negative correlation was observed between FFV and percent conversion, implying that polymer chains are densifying through viscous conformational rearrangement to occupy the newly formed free volume elements. At similar conversions, samples treated at $130\text{ }^{\circ}\text{C}$ generally exhibited higher FFV than samples treated at $140\text{ }^{\circ}\text{C}$ and $160\text{ }^{\circ}\text{C}$. While t-BOC-160-5min and t-BOC-130-1h had similar conversions, the FFV value of t-BOC-130-1h was higher and had a comparable value to that of 6FDA-HAB-t-BOC. This finding reveals that higher temperatures induce more chain mobility and faster kinetics for the reorganization of the packed polymer structure, accelerating the reduction in FFV. While FFV was unchanged between the BOC protected sample and the samples treated at $130\text{ }^{\circ}\text{C}$ for either 1 or 2 h, there were no indications of increased FFV during the porogen removal process.

Holding samples for 16 h at all three temperatures resulted in identical FFV values within the uncertainty of our analysis procedure. As previously noted in **Table 2**, these samples all had

identical conversions, and when compared to 6FDA-HAB, all samples had the same values of FFV. These findings indicate that the ensemble of packing structures accessible to these three samples average to approximately the same FFV as that determined for 6FDA-HAB.

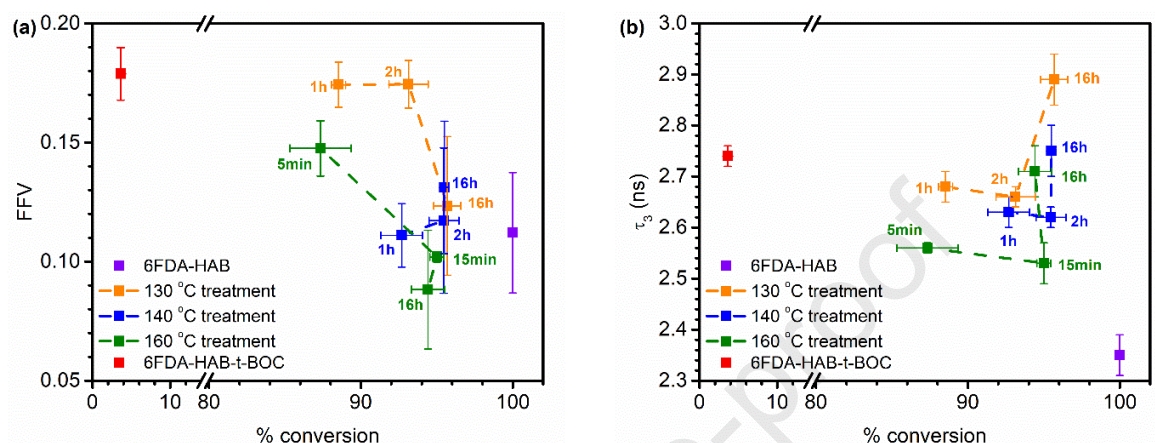


Figure 4: Percent conversion (from 6FDA-HAB-t-BOC to 6FDA-HAB) compared to (a) FFV and (b) τ_3 for all samples in this study. Thermally treated samples are labeled with their treatment times. Dashed lines have been added to guide the eye and are not representative of a predictive relationship.

While useful in estimating many bulk properties of polymers, because group contribution methods are compiled by averaging massive datasets, molecular-level details are often obscured by this approach [60,63]. Therefore, conclusions drawn from **Figure 4a** in regards to changes in polymer structure should be taken with caution, as FFV measurements from group contribution methods provide no direct indication of the free volume distribution. Instead, we used PALS to more accurately track changes in free volume and determine if trends derived from group contribution methods were relevant for analyzing this series of polymers. While certain high free volume polymers, such as PIMs, can be fit to PALS data using bimodal free volume size distributions [13,64–66], a unimodal fit was found to most accurately represent all polymers in

this study, implying that deprotection did not create discrete free volume elements of significant intensity.

A graphical comparison of percent conversion versus τ_3 is presented in **Figure 4b**. Consistent with our FFV findings, PALS revealed that 6FDA-HAB displayed a smaller average τ_3 than that of 6FDA-HAB-t-BOC. In general, higher temperatures and longer treatment times resulted in smaller τ_3 values, and hence, reduced free volume element sizes, which aligns with our FFV interpretation. However, one notable difference was observed for τ_3 values for all 16 h treatments, regardless of treatment temperatures considered. Of note, t-BOC-130-16h contains free volume elements that are larger than those of 6FDA-HAB-t-BOC. This counterintuitive result is in contrast to trends derived from FFV and requires further investigation.

Three major possibilities exist to explain these findings. The first relates to slow diffusion of t-BOC decomposition products, the second relates to casting solvents and thermal conditioning, and the third relates to evidence of successful, albeit limited evidence of free volume manipulation. The first two possibilities are discussed here, and the third possibility is discussed in Section 3.4. As previously described, trace amounts of isobutylene are formed in the 6FDA-HAB-t-BOC polymer films as they undergo thermal deprotection. Although the presence of isobutylene is no longer detectable by NMR for many of our samples, it is possible that trace amounts of isobutylene conceal some limited anisotropy in the free volume packing structure of our polymers. Olefinic species, which are electron-rich, are known to inhibit positronium formation [52], so small contributions of trapped isobutylene could inhibit the clear detection of porogen features. However, we expect these considerations to be minimal in our samples since any residual isobutylene remaining in each film would be vastly insufficient to occupy all of the porogen domains, but such an effect could explain the slight increase in τ_3 values for all of the

16 h thermally treated samples, which would correspondingly have the lowest content of isobutylene.

The second possibility relates to casting solvents and thermal conditioning. For casting solvents, this consideration only applies for comparisons with 6FDA-HAB because this polymer could only be cast from high boiling point solvents, as discussed previously. All comparisons between deprotected analogues of 6FDA-HAB-t-BOC are fully self-consistent, since all of these samples underwent identical solvent removal procedures. Along these lines, changes in polymer packing structure due to different casting solvents have been noted previously, especially for high free volume polymers [67], but the 16 h treatments were done consistently to 6FDA-HAB-t-BOC samples cast from identical solvents. Therefore, it is unlikely that the differences in τ_3 values could be attributed to solvent effects. Instead, these differences are much more likely related to slight differences in thermal annealing temperatures, as will be discussed in Section 3.4.

Despite the weak correlations in **Figure 4a** and **4b**, several conclusions can be made about applying the porogen approach to linear polyimides that have high T_g . Most importantly, exposure to elevated temperatures can sufficiently induce mobility of the 6FDA-HAB polymer matrix, causing both FFV and average free volume element size to decrease with increasing treatment temperature. As t-BOC is thermally removed, the regeneration of hydroxyl functional groups further induces matrix densification, as new opportunities for hydrogen bonding result [68,69]. Moreover, polymer relaxation processes appear to occur well below the T_g . Comer et al. have demonstrated the presence of sub- T_g transitions occurring for 6FDA-HAB around 150 °C [70], so while long-range cooperative motion is suppressed below the T_g , these sub- T_g motions may result in the collapse of the newly created porogen architecture. In view of these complexities, while we conclude that the removal of t-BOC generates free volume elements, the

generation of such free volume elements drives the polymer further away from its theoretical chain packing equilibrium structure, which accelerates physical aging according to the Struik Model [71], leading to the reorganization of polymer chains upon t-BOC removal induced by high temperature.

3.4. Effect of sample treatment on gas transport properties

The pure-gas permeabilities of He, H₂, CH₄, N₂, O₂, and CO₂ for all polymer films are tabulated in **Table 4**. Diffusion and sorption coefficients are also summarized in **Table 4**, and permselectivities of select gas pairs are shown in **Table 5**. A graphical comparison of percent conversion versus permeability for all six gases is presented in Figure S7. Analogous plots for diffusion and sorption coefficients for N₂, O₂, CH₄, and CO₂ are shown in Figures S8 and S9, respectively. Plots of diffusion coefficient versus effective diameter squared and sorption coefficient versus critical temperature for all samples are also included in Figures S10 and S11, respectively. Diffusion coefficients in all samples increased as follows: $D(\text{CH}_4) < D(\text{CO}_2) \sim D(\text{N}_2) < D(\text{O}_2)$, which follows the inverse order of effective diameter ((3.44 Å) O₂ < (3.63 Å) CO₂ ~ (3.66 Å) N₂ < (3.81 Å) CH₄), as expected for glassy polymers. Gas sorption coefficients in all samples increased with increasing critical temperatures of penetrant molecules as follows: $S(\text{N}_2) < S(\text{O}_2) < S(\text{CH}_4) < S(\text{CO}_2)$, which follows gas sorption trends for other polymers [72].

Table 4: Pure-gas permeabilities (P), diffusion coefficients (D), and solubility coefficients (S) for 6FDA-HAB, 6FDA-HAB-t-BOC, and 6FDA-HAB-t-BOC after various thermal treatments

Sample	Treatment Temperature (°C)	Hold time		He	H ₂	N ₂	O ₂	CH ₄	CO ₂
6FDA-HAB	n/a	n/a	P	53 ± 4	42 ± 3	0.37 ± 0.03	2.6 ± 0.2	0.17 ± 0.01	12.3 ± 0.9
			D	/	/	5.9 ± 0.8	28 ± 4	0.70 ± 0.05	6.5 ± 0.9
			S	/	/	0.47 ± 0.07	0.7 ± 0.1	1.8 ± 0.3	14 ± 2
6FDA-HAB-t-BOC	n/a	n/a	P	64 ± 2	61 ± 2	1.89 ± 0.05	8.4 ± 0.3	1.61 ± 0.05	42 ± 1
			D	/	/	40 ± 2	142 ± 8	10.9 ± 0.4	37 ± 2
			S	/	/	0.36 ± 0.02	0.45 ± 0.03	1.13 ± 0.09	8.7 ± 0.5
6FDA-HAB-t-BOC	130	1 h	P	59 ± 4	56 ± 4	1.09 ± 0.08	5.8 ± 0.4	0.49 ± 0.04	32 ± 2
			D	/	/	14 ± 2	63 ± 9	2.5 ± 0.2	14 ± 2
			S	/	/	0.6 ± 0.1	0.7 ± 0.1	1.5 ± 0.2	17 ± 3
		2 h	P	54 ± 5	51 ± 5	1.1 ± 0.1	4.7 ± 0.4	0.80 ± 0.08	24 ± 2
			D	/	/	14 ± 3	45 ± 9	2.6 ± 0.4	11 ± 2
			S	/	/	0.6 ± 0.1	0.8 ± 0.2	2.3 ± 0.3	17 ± 4
		16 h	P	51 ± 3	46 ± 3	0.55 ± 0.04	3.4 ± 0.2	0.22 ± 0.02	18 ± 1
			D	/	/	6.4 ± 0.9	29 ± 4	0.60 ± 0.06	7 ± 1
			S	/	/	0.7 ± 0.1	0.9 ± 0.1	2.8 ± 0.4	19 ± 3
6FDA-HAB-t-BOC	140	1 h	P	54 ± 5	50 ± 5	0.75 ± 0.07	4.2 ± 0.4	0.33 ± 0.03	22 ± 2
			D	/	/	11 ± 2	48 ± 9	1.2 ± 0.2	12 ± 2
			S	/	/	0.5 ± 0.1	0.7 ± 0.1	2.1 ± 0.4	15 ± 3
		2 h	P	66 ± 3	58 ± 2	0.73 ± 0.03	4.4 ± 0.2	0.26 ± 0.01	22.7 ± 0.9
			D	/	/	6.5 ± 0.5	34 ± 3	0.81 ± 0.04	8.3 ± 0.7
			S	/	/	0.85 ± 0.08	0.97 ± 0.09	2.4 ± 0.2	21 ± 2
		16 h	P	53 ± 2	46 ± 1	0.50 ± 0.02	3.1 ± 0.1	0.183 ± 0.007	15.5 ± 0.5
			D	/	/	5.4 ± 0.3	26 ± 2	0.48 ± 0.02	7.0 ± 0.4
			S	/	/	0.70 ± 0.05	0.91 ± 0.06	2.9 ± 0.2	17 ± 1
6FDA-HAB-t-BOC	160	5 min	P	59 ± 5	58 ± 5	1.5 ± 0.1	7.5 ± 0.6	1.05 ± 0.09	45 ± 4
			D	/	/	27 ± 5	100 ± 20	4.7 ± 0.8	28 ± 6
			S	/	/	0.42 ± 0.09	0.6 ± 0.1	1.7 ± 0.3	12 ± 3
		15 min	P	61 ± 4	57 ± 4	0.87 ± 0.05	5.0 ± 0.3	0.37 ± 0.03	27 ± 2
			D	/	/	11 ± 2	47 ± 6	1.4 ± 0.1	13 ± 2
			S	/	/	0.58 ± 0.09	0.8 ± 0.1	2.0 ± 0.2	16 ± 2
		16 h	P	48 ± 1	40.6 ± 0.9	0.43 ± 0.01	2.83 ± 0.07	0.164 ± 0.005	13.9 ± 0.3
			D	/	/	5.6 ± 0.2	27 ± 1	0.58 ± 0.02	7.0 ± 0.3
			S	/	/	0.58 ± 0.03	0.80 ± 0.04	2.2 ± 0.1	15.1 ± 0.7

Units: P (barrer = 10^{-10} cm³(STP) cm cm⁻² s⁻¹ cmHg⁻¹ or 3.348×10^{-16} mol m m⁻² s⁻¹ Pa⁻¹), D (10⁻⁹ cm² s⁻¹), S (cm³(STP) cm⁻³ atm⁻¹).

Table 5: Ideal permselectivities of select gas pairs for 6FDA-HAB, 6FDA-HAB-t-BOC, and 6FDA-HAB-t-BOC after various thermal treatments.

Sample	Treatment Temperature (°C)	Hold time	O ₂ /N ₂	CO ₂ /CH ₄	CO ₂ /N ₂	H ₂ /CH ₄	N ₂ /CH ₄
6FDA-HAB	n/a	n/a	7.1 ± 0.7	74 ± 8	34 ± 3	250 ± 30	2.2 ± 0.2
6FDA-HAB-t-BOC	n/a	n/a	4.4 ± 0.2	26 ± 1	22 ± 1	38 ± 2	1.18 ± 0.05
6FDA-HAB-t-BOC	130	1 h	5.3 ± 0.5	66 ± 8	29 ± 3	120 ± 10	2.3 ± 0.3
		2 h	4.2 ± 0.6	30 ± 4	21 ± 3	64 ± 9	1.4 ± 0.2
		16 h	6.3 ± 0.6	80 ± 8	32 ± 3	210 ± 20	2.5 ± 0.3
6FDA-HAB-t-BOC	140	1 h	5.7 ± 0.7	67 ± 9	30 ± 4	150 ± 20	2.2 ± 0.3
		2 h	6.0 ± 0.4	89 ± 6	31 ± 2	230 ± 20	2.9 ± 0.2
		16 h	6.3 ± 0.3	85 ± 4	31 ± 1	250 ± 10	2.7 ± 0.1
6FDA-HAB-t-BOC	160	5 min	5.0 ± 0.6	42 ± 5	30 ± 4	55 ± 7	1.4 ± 0.2
		15 min	5.7 ± 0.5	72 ± 7	31 ± 3	150 ± 10	2.4 ± 0.2
		16 h	6.6 ± 0.2	85 ± 3	32 ± 1	248 ± 9	2.6 ± 0.1

As shown in **Table 4**, the permeabilities of all six gases tested for 6FDA-HAB-t-BOC are higher than those for 6FDA-HAB, while the selectivities for all gas pairs considered are lower. This increase in gas permeability is consistent with FFV and PALS data and suggests that the bulky t-BOC functional groups in 6FDA-HAB-t-BOC lead to less efficient polymer chain packing in the films. Moreover, diffusion coefficients in 6FDA-HAB-t-BOC are significantly higher than those in 6FDA-HAB, which is again consistent with the FFV and PALS data, as the t-BOC group can act as a bulky spacer to further expand the free volume and allow for increased gas diffusion [73]. These results are in accordance with the expected exponential correlation between fractional free volume and diffusion coefficients, $D = A \exp(-\frac{B}{FFV})$, where A and B are adjustable parameters [59,74–77]. However, sorption coefficients for 6FDA-HAB-t-BOC are lower than those for 6FDA-HAB, which is likely due to the presence of polar hydroxyl functional groups which can enhance chemical affinity of molecular diluents. The inclusion of polar functionality has led to increases in sorption for other polymers such as cellulose acetate [78], poly(methyl methacrylate) (PMMA) [78], polysulfone [79], and PIM-1 [80]. Since the difference in diffusion coefficients is more pronounced than the difference in sorption

coefficients, there is an overall increase in permeability for 6FDA-HAB-t-BOC compared to 6FDA-HAB.

In order to visualize the effects of different thermal treatments on gas transport properties, Robeson upper bound plots for O_2/N_2 and CO_2/CH_4 gas pairs are shown in **Figure 5**. Additional Robeson plots for other gas pairs listed in **Table 5** can be found in Section S4. As the t-BOC group is removed, permeability generally decreases and selectivity increases, implying that discrete free volume elements are not maintained. However, permeability is the product of sorption and diffusion, and a successful application of free volume manipulation would imply increases in diffusion as free volume is created by porogen removal.

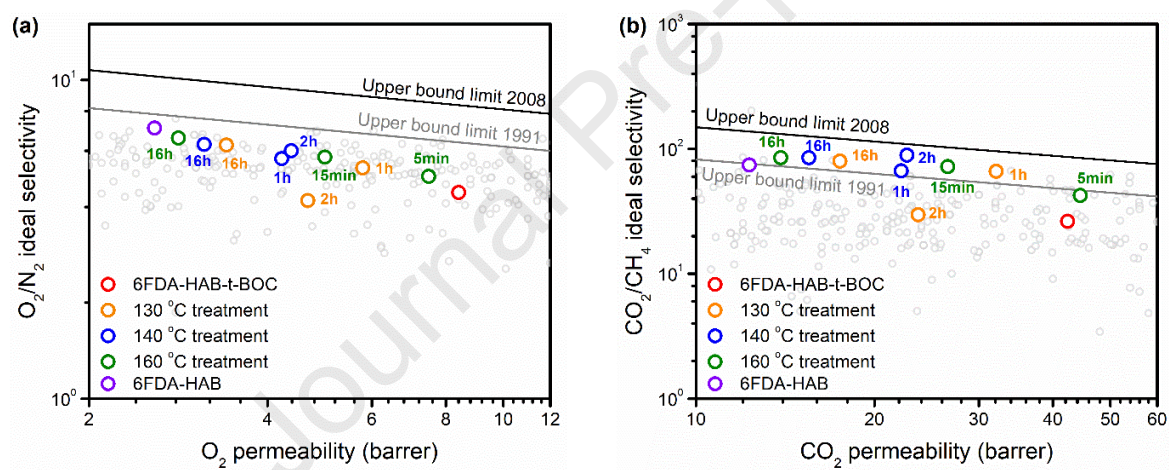


Figure 5: Robeson upper bound plots for a) O_2/N_2 , and b) CO_2/CH_4 gas pairs. Thermally treated samples are labeled with their treatment times. The black and gray lines represent the 2008 and 1991 Robeson upper bounds, respectively [81,82]. Literature data are shown as open gray circles from Robeson's database [81,82].

At each temperature treatment, as t-BOC is removed, permeabilities and diffusion coefficients generally decrease and approach those of 6FDA-HAB, while both sorption coefficients and permselectivities of all considered gas pairs generally increase. While these

trends indicate significant free volume reorganization, there are a few notable exceptions to these trends, and for the samples treated at 16 h, differences in FFV calculations and τ_3 values. These differences may indicate some limited evidence of FVM. Additionally, differences in free volume distribution could also explain how some samples (notably, t-BOC-130-16h, t-BOC-140-2h, and t-BOC-140-16h) have sorption coefficients that are higher than those for 6FDA-HAB, despite being chemically similar.

To investigate evidence of FVM, we turn to a few samples that exhibited morphological characteristics and/or transport effects that could support this interpretation. t-BOC-130-2h, in particular, was treated for a longer time than t-BOC-130-1h, yet the former possesses a lower selectivity for all gas pairs considered. In addition, the CH_4 permeability of t-BOC-130-2h (0.80 barrer) is higher than that of t-BOC-130-1h (0.49 barrer). These results can be explained by decoupling the permeability into diffusion and sorption coefficients. While t-BOC-130-1h and t-BOC-130-2h have identical CH_4 diffusion coefficients, the CH_4 sorption coefficient of t-BOC-130-2h ($2.3 \text{ cm}^3(\text{STP}) \text{ cm}^{-3} \text{ atm}^{-1}$) is higher than that of t-BOC-130-1h ($1.5 \text{ cm}^3(\text{STP}) \text{ cm}^{-3} \text{ atm}^{-1}$), which can be attributed to the higher conversion of t-BOC-130-2h ($93\% \pm 1\%$) compared to t-BOC-130-1h ($88.5\% \pm 0.5\%$). Because the FFV and τ_3 values are identical for these samples, differences in transport properties are governed by sorption effects and not indicative of significant FVM.

Another notable exception to the general trends was observed for t-BOC-140-1h and t-BOC-140-2h. Specifically, both the H_2 and He permeability coefficients of t-BOC-140-2h (66 and 58 barrer, respectively) are higher than those for t-BOC-140-1h (54 and 50 barrer, respectively). This result leads to a higher H_2/CH_4 selectivity for t-BOC-140-2h. For larger gases, diffusion coefficients decrease as treatment time at 140 °C increases, which correlates with the

systematic decrease in I_3 , indicating a reduction in the number of free volume elements. However, O_2 , N_2 , and CO_2 sorption coefficients for t-BOC-140-2h exceed those for t-BOC-140-1h, even though the percent conversion, FFV, and τ_3 values are equivalent between the two samples. In addition, the sorption coefficients of all gases considered for t-BOC-140-2h exceed those for 6FDA-HAB. While t-BOC-140-2h can be considered chemically equivalent to 6FDA-HAB due to its conversion ($95\% \pm 1\%$), the τ_3 value of t-BOC-140-2h is $11\% \pm 2\%$ larger than that of 6FDA-HAB. A larger τ_3 value correlates with a larger average free volume element size, which indicates the presence of some excess volume in t-BOC-140-2h that does not exist in the directly formed 6FDA-HAB film. Since Robeson et al. have shown that excess free volume in polymers has a weak influence on sorption [83], it is likely that the excess free volume found in t-BOC-140-2h contributes to higher sorption coefficients. While sorption coefficients for He and H_2 could not be determined, we would anticipate significantly higher sorption coefficients and permeabilities for these smaller gases in t-BOC-140-2h relative to 6FDA-HAB. While the effect is relatively small, these findings indicate some evidence of FVM for the 140 °C series. As one caveat, we refer to our earlier discussion on PALS results, where bimodal free volume distributions could not be fit for these samples. Therefore, conclusions of successful FVM in this series are somewhat nuanced, because sorption clearly increases from t-BOC-140-1h to t-BOC-140-2h, but both samples have similar FFV and τ_3 values.

Treatment temperatures of both 130 °C and 140 °C are below the prominent deprotection temperature of t-BOC, but the treatment temperature of 160 °C allows for the effects of faster deprotection on polymer chain rearrangement to be studied. When comparing samples that have similar conversions but different treatment conditions, it was generally found that with higher deprotection temperatures and longer treatment times, gas permeability decreases, coupled with

increases in selectivity. In particular, samples treated at 160 °C for significantly shorter times (5 min and 15 min) yield comparable gas transport results to those treated at 130 °C and 140 °C for longer times (1 h and 2 h). Although lower FFV values at similar conversions generally result in lower permeability, some exceptions were found that require further investigation. For example, while t-BOC-160-5min has a lower τ_3 value than t-BOC-130-1h, permeabilities for N₂, O₂, CH₄, and CO₂ are higher. This difference in permeability is mainly attributed to diffusion. A similar case is observed between t-BOC-140-2h and t-BOC-160-15min, in which the latter sample possesses a lower τ_3 value but higher permeabilities and diffusion coefficients for N₂, O₂, CH₄, and CO₂. The nearly equivalent FFV values between t-BOC-130-1h and t-BOC-160-5min and between t-BOC-140-2h and t-BOC-160-15min suggest that the free volume distribution between the two sample pairs differs, although these differences are again notably small.

As a final comparison, there are limited variations in diffusion coefficients for all four gases measured among the three samples annealed for 16 h. The independence of temperature on diffusion coefficients at a treatment time of 16 h is particularly interesting, as previous studies have shown that higher temperature treatments on polymer films can lead to larger decreases in diffusion coefficients [69]. There is a possibility that at 16 h, thermally-treated 6FDA-HAB-t-BOC has reached a state in which additional time may not warrant any obvious effects on the packing structure [35]. Such an interpretation would suggest that sub- T_g transitions, which are known to exist in 6FDA-HAB at our annealing temperatures [70], have had sufficient time to reorganize the polymer packing structure such that the porogen templates have effectively been removed from the polymer matrix. A further study that examines the three thermal treatment temperatures used for times longer than 2 h, but shorter than 16 h, may elucidate this phenomenon.

4. Conclusions

In this study, the effect of thermal deprotection reactions on free volume manipulation (FVM) and gas transport properties was investigated. The control sample, 6FDA-HAB, was functionalized with t-BOC substituents to generate 6FDA-HAB-t-BOC, which was then cast into films. These films were subjected to thermal treatment conditions at various temperatures and times to study the effects of treatment conditions on polymer packing structure. Results were evaluated using FFV, PALS, and gas transport properties. Because deprotection reactions were all significantly below the glass transition temperature of 6FDA-HAB, we hypothesized that this method of FVM could generate free volume elements that were approximately the size of t-BOC. However, the results were far more nuanced, indicating that the thermally deprotected polymer underwent sufficient structural reorganization during thermal treatments, and complete retention of the created free volume elements could not be fully preserved. While certain samples showed some limited evidence of successful FVM, after sufficient thermal treatment, transport properties and physical characteristics of the deprotected samples closely resembled those of pure 6FDA-HAB. Extensive synthetic methods and characterization experiments demonstrate how this deprotection approach can be applied to high- T_g polymers with functional groups that can be protected. Applying these approaches to polymers with more restricted chain mobilities may enable more extensive manipulation and control to generate free volume elements from this top-down FVM approach.

Acknowledgements

This work was supported by the U.S. Department of Energy, Office of Science, Office of Basic Energy Sciences, Separation Science program under Award Number DE-SC0019087. F. M.

Benedetti was supported by the MIT Energy Initiative as part of the Society of Energy Fellows at MIT. A. X. Wu was supported by NSF-GRFP (DGE-1122374) and K. Mizrahi Rodriguez was supported through a Ford Foundation Pre-Doctoral Fellowship administered by the National Academies of Science Engineering and Medicine. The authors would like to thank Professor Matthew Hill and members of the Hill group at Monash University for use of lab space and stimulating discussions. The authors would also like to thank Professor Douglass S. Kalika at University of Kentucky for useful discussions. The authors would also like to give special thanks to members of the Smith group at the Massachusetts Institute of Technology for their valuable help.

Appendix A. Supplementary data

The supplementary data associated in this article can be found in the online version at (DOI).

References

- [1] D.F. Sanders, Z.P. Smith, R. Guo, L.M. Robeson, J.E. McGrath, D.R. Paul, B.D. Freeman, Energy-efficient polymeric gas separation membranes for a sustainable future: A review, *Polymer* 54 (2013) 4729–4761.
- [2] R.W. Baker, Future directions of membrane gas separation technology, *Ind. Eng. Chem. Res.* 41 (2002) 1393–1411.
- [3] M. Galizia, W.S. Chi, Z.P. Smith, T.C. Merkel, R.W. Baker, B.D. Freeman, 50th anniversary perspective: Polymers and mixed matrix membranes for gas and vapor separation: a review and prospective opportunities, *Macromolecules* 50 (2017) 7809–7843.
- [4] T. Corrado, R. Guo, Macromolecular design strategies toward tailoring free volume in glassy polymers for high performance gas separation membranes, *Mol. Syst. Des. Eng.* 5 (2020) 22–48.
- [5] I. Rose, C.G. Bezzu, M. Carta, B. Comesanã-Gándara, E. Lasseuguette, M.C. Ferrari, P. Bernardo, G. Clarizia, A. Fuoco, J.C. Jansen, K.E. Hart, T.P. Liyana-Arachchi, C.M. Colina, N.B. McKeown, Polymer ultrapermeability from the inefficient packing of 2D chains, *Nat. Mater.* 16 (2017) 932–937.
- [6] B. Comesaña-Gándara, J. Chen, C.G. Bezzu, M. Carta, I. Rose, M.-C. Ferrari, E. Esposito, A. Fuoco, J.C. Jansen, N.B. McKeown, Redefining the Robeson upper bounds for CO₂/CH₄ and CO₂/N₂ separations using a series of ultrapermeable benzotriptycene-based polymers of intrinsic microporosity, *Energy Environ. Sci.* 12 (2019) 2733–2740.
- [7] P.M. Budd, E.S. Elabas, B.S. Ghanem, S. Makhseed, N.B. McKeown, K.J. Msayib, C.E. Tattershall, D. Wang, Solution-Processed, Organophilic membrane derived from a

- polymer of intrinsic microporosity, *Adv. Mater.* 16 (2004) 456–459.
- [8] M. Carta, M. Croad, R. Malpass-Evans, J.C. Jansen, P. Bernardo, G. Clarizia, K. Friess, M. Lanč, N.B. McKeown, Triptycene induced enhancement of membrane gas selectivity for microporous Tröger's base polymers, *Adv. Mater.* 26 (2014) 3526–3531.
- [9] J.R. Wiegand, Z.P. Smith, Q. Liu, C.T. Patterson, B.D. Freeman, R. Guo, Synthesis and characterization of triptycene-based polyimides with tunable high fractional free volume for gas separation membranes, *J. Mater. Chem. A* 2 (2014) 13309–13320.
- [10] M. Carta, R. Malpass-Evans, M. Croad, Y. Rogan, J.C. Jansen, P. Bernardo, F. Bazzarelli, N.B. McKeown, An efficient polymer molecular sieve for membrane gas separations, *Science* 339 (2013) 303–307.
- [11] H.B. Park, C.H. Jung, Y.M. Lee, A.J. Hill, S.J. Pas, S.T. Mudie, E. Van Wagner, B.D. Freeman, D.J. Cookson, Polymers with cavities tuned for fast selective transport of small molecules and ions, *Science* 318 (2007) 254–258.
- [12] Z.P. Smith, G. Hernández, K.L. Gleason, A. Anand, C.M. Doherty, K. Konstas, C. Alvarez, A.J. Hill, A.E. Lozano, D.R. Paul, B.D. Freeman, Effect of polymer structure on gas transport properties of selected aromatic polyimides, polyamides and TR polymers, *J. Memb. Sci.* 493 (2015) 766–781.
- [13] S.H. Han, N. Misdan, S. Kim, C.M. Doherty, A.J. Hill, Y.M. Lee, Thermally rearranged (TR) polybenzoxazole: Effects of diverse imidization routes on physical properties and gas transport behaviors, *Macromolecules* 43 (2010) 7657–7667.
- [14] S.A. MacDonald, C.G. Willson, J.M.J. Fréchet, Chemical amplification in high-resolution

- imaging systems, *Acc. Chem. Res.* 27 (1994) 151–158.
- [15] T. Omote, K. Koseki, T. Yamaoka, Fluorine-containing photoreactive polyimides. 6. Synthesis and properties of a novel photoreactive polyimide based on photo-induced acidolysis and the kinetics for its acidolysis, *Macromolecules* 23 (1990) 4788–4795.
- [16] T. Fukumaru, T. Fujigaya, N. Nakashima, Design and preparation of porous polybenzoxazole films using the tert-butoxycarbonyl group as a pore generator and their application for patternable low-k materials, *Polym. Chem.* 3 (2012) 369–376.
- [17] S. Merlet, C. Marestin, O. Romeyer, R. Mercier, “Self-foaming” poly(phenylquinoxaline)s for the designing of macro and nanoporous materials, *Macromolecules* 41 (2008) 4205–4215.
- [18] S. Merlet, C. Marestin, F. Schiets, O. Romeyer, R. Mercier, Preparation and characterization of nanocellular poly(phenylquinoxaline) foams. A new approach to nanoporous high-performance polymers, *Macromolecules* 40 (2007) 2070–2078.
- [19] Y. Xiao, T.S. Chung, Grafting thermally labile molecules on cross-linkable polyimide to design membrane materials for natural gas purification and CO₂ capture, *Energy Environ. Sci.* 4 (2011) 201–208.
- [20] M. Askari, M.L. Chua, T.S. Chung, Permeability, solubility, diffusivity, and PALS data of cross-linkable 6FDA-based copolyimides, *Ind. Eng. Chem. Res.* 53 (2014) 2449–2460.
- [21] M. Askari, Y. Xiao, P. Li, T.S. Chung, Natural gas purification and olefin/paraffin separation using cross-linkable 6FDA-Durene/DABA co-polyimides grafted with α , β , and γ -cyclodextrin, *J. Memb. Sci.* 390–391 (2012) 141–151.

- [22] M.L. Chua, Y.C. Xiao, T. Chung, Effects of thermally labile saccharide units on the gas separation performance of highly permeable polyimide membranes, *J. Memb. Sci.* 415–416 (2012) 375–382.
- [23] M.N. Islam, W. Zhou, T. Honda, K. Tanaka, H. Kita, K.I. Okamoto, Preparation and gas separation performance of flexible pyrolytic membranes by low-temperature pyrolysis of sulfonated polyimides, *J. Memb. Sci.* 261 (2005) 17–26.
- [24] W. Zhou, T. Watari, H. Kita, K.I. Okamoto, Gas permeation properties of flexible pyrolytic membranes from sulfonated polyimides, *Chem. Lett.* (2002) 534–535.
- [25] E.M. Maya, A. Tena, J. de Abajo, J.G. de la Campa, A.E. Lozano, Partially pyrolyzed membranes (PPMs) derived from copolyimides having carboxylic acid groups. Preparation and gas transport properties, *J. Memb. Sci.* 349 (2010) 385–392.
- [26] E. Martínez-Mercado, F.A. Ruiz-Treviño, A. Cruz-Rosado, M.G. Zolotukhin, A. González-Montiel, J. Cárdenas, R.L. Gaviño-Ramírez, Tuning gas permeability and selectivity properties by thermal modification of the side groups of poly(oxindolebiphenylene)s membranes, *Ind. Eng. Chem. Res.* 53 (2014) 15755–15762.
- [27] S. Zheng, L.M. Robeson, M.K. Murphy, J.R. Quay, Polymers, polymer membranes and methods of producing the same, US Patent 8926733B2 (2015).
- [28] S. Sánchez-García, F.A. Ruiz-Treviño, M.J. Aguilar-Vega, M.G. Zolotukhin, Gas permeability and selectivity in thermally modified poly(oxyindole biphenylene) membranes bearing a tert-butyl carbonate group, *Ind. Eng. Chem. Res.* 55 (2016) 7012–7020.

- [29] H. Hernández-Martínez, F.A. Ruiz-Treviño, J. Ortiz-Espinoza, M.J. Aguilar-Vega, M.G. Zolotukhin, R. Marcial-Hernandez, L.I. Olvera, Simultaneous thermal cross-linking and decomposition of side groups to mitigate physical aging in poly(oxyindole biphenylene) gas separation membranes, *Ind. Eng. Chem. Res.* 57 (2018) 4640–4650.
- [30] C.H. Ho, T. Vu-Khanh, Effects of time and temperature on physical aging of polycarbonate, *Theor. Appl. Fract. Mech.* 39 (2003) 107–116.
- [31] Y. Huang, D.R. Paul, Physical aging of thin glassy polymer films monitored by gas permeability, *Polymer* 45 (2004) 8377–8393.
- [32] Y. Huang, D.R. Paul, Effect of temperature on physical aging of thin glassy polymer films, *Macromolecules* 38 (2005) 10148–10154.
- [33] L.A.G. Gray, S.W. Yoon, W.A. Pahner, J.E. Davidheiser, C.B. Roth, Importance of quench conditions on the subsequent physical aging rate of glassy polymer films, *Macromolecules* 45 (2012) 1701–1709.
- [34] H. Wang, T.S. Chung, D.R. Paul, Physical aging and plasticization of thick and thin films of the thermally rearranged ortho-functional polyimide 6FDA–HAB, *J. Memb. Sci.* 458 (2014) 27–35.
- [35] L. Ansaloni, M. Minelli, M.G. Baschetti, G.C. Sarti, Effects of thermal treatment and physical aging on the gas transport properties in Matrimid®, *Oil Gas Sci. Technol.* 70 (2015) 367–379.
- [36] K. Tanaka, H. Kita, M. Okano, K. Okamoto, Permeability and permselectivity of gases in fluorinated polyimides, *Polymer* 33 (1992) 585–592.

- [37] S.A. Stern, Y. Mi, H. Yamamoto, A.K. St. Clair, Structure/permeability relationships of polyimide membranes. Applications to the separation of gas mixtures, *J. Polym. Sci. Part B Polym. Phys.* 27 (1989) 1887–1909.
- [38] T.H. Kim, W.J. Koros, G.R. Husk, K.C. O'Brien, Relationship between gas separation properties and chemical structure in a series of aromatic polyimides, *J. Memb. Sci.* 37 (1988) 45–62.
- [39] W. Qiu, L. Xu, C.C. Chen, D.R. Paul, W.J. Koros, Gas separation performance of 6FDA-based polyimides with different chemical structures, *Polymer* 54 (2013) 6226–6235.
- [40] Z.P. Smith, D.F. Sanders, C.P. Ribeiro, R. Guo, B.D. Freeman, D.R. Paul, J.E. McGrath, S. Swinnea, Gas sorption and characterization of thermally rearranged polyimides based on 3,3'-dihydroxy-4,4'-diamino-biphenyl (HAB) and 2,2'-bis-(3,4-dicarboxyphenyl) hexafluoropropane dianhydride (6FDA), *J. Memb. Sci.* 415–416 (2012) 558–567.
- [41] D.F. Sanders, Z.P. Smith, C.P. Ribeiro, R. Guo, J.E. McGrath, D.R. Paul, B.D. Freeman, Gas permeability, diffusivity, and free volume of thermally rearranged polymers based on 3,3'-dihydroxy-4,4'-diamino-biphenyl (HAB) and 2,2'-bis-(3,4-dicarboxyphenyl) hexafluoropropane dianhydride (6FDA), *J. Memb. Sci.* 409–410 (2012) 232–241.
- [42] R. Guo, D.F. Sanders, Z.P. Smith, B.D. Freeman, D.R. Paul, J.E. McGrath, Synthesis and characterization of thermally rearranged (TR) polymers: influence of ortho-positioned functional groups of polyimide precursors on TR process and gas transport properties, *J. Mater. Chem. A* 1 (2013) 262–272.
- [43] D.F. Sanders, R. Guo, Z.P. Smith, Q. Liu, K.A. Stevens, J.E. McGrath, D.R. Paul, B.D. Freeman, Influence of polyimide precursor synthesis route and ortho-position functional

- group on thermally rearranged (TR) polymer properties: Conversion and free volume, *Polymer* 55 (2014) 1636–1647.
- [44] A.J. Hill, Positron annihilation lifetime spectroscopy, in: G.P. Simon (Ed.), *Polymer Characterization Techniques and Their Applications to Blends*, Oxford University Press, Washington, DC, 2003, pp. 401–435.
- [45] J.R. Weidman, S. Luo, C.M. Doherty, A.J. Hill, P. Gao, R. Guo, Analysis of governing factors controlling gas transport through fresh and aged triptycene-based polyimide films, *J. Memb. Sci.* 522 (2017) 12–22.
- [46] R.A. Pethrick, Positron annihilation—A probe for nanoscale voids and free volume?, *Prog. Polym. Sci.* 22 (1997) 1–47.
- [47] M. Askari, M.L. Chua, T. Chung, Permeability, solubility, diffusivity, and PALS data of cross-linkable 6FDA-based copolyimides, *Ind. Eng. Chem. Res.* 53 (2014) 2449–2460.
- [48] R.W. Siegel, Positron annihilation spectroscopy, *Annu. Rev. Mater. Sci.* 10 (1980) 393–425.
- [49] J. Kansy, Microcomputer program for analysis of positron annihilation lifetime spectra, *Nucl. Instrum. Methods Phys. Res. Sect. A.* 374 (1996) 235–244.
- [50] S.J. Tao, Positronium annihilation in molecular substances, *J. Chem. Phys.* 56 (1972) 5499–5510.
- [51] M. Eldrup, D. Lightbody, J.N. Sherwood, The temperature dependence of positron lifetimes in solid pivalic acid, *Chem. Phys.* 63 (1981) 51–58.
- [52] Y.C. Jean, P.E. Mallon, D.M. Schrader, *Principles and Applications of Positron &*

- Positronium Chemistry, World Scientific, Singapore, 2003.
- [53] V.P. Shantarovich, T. Suzuki, C. He, V.W. Gustov, Inhibition of positronium formation by polar groups in polymers—relation with TSL experiments, *Radiat. Phys. Chem.* 67 (2003) 15–23.
- [54] H. Lin, B.D. Freeman, Permeation and diffusion, in: H. Czichos, T. Saito, L. Smith (Eds.), *Springer Handbook of Materials Measurement Methods*, Springer Berlin Heidelberg Berlin, Heidelberg, 2006, pp. 371–387.
- [55] H.L. Frisch, The time lag in diffusion, *J. Phys. Chem.* 61 (1957) 93–95.
- [56] J.G. Wijmans, R.W. Baker, The solution-diffusion model: a review, *J. Memb. Sci.* 107 (1995) 1–21.
- [57] P.R. Bevington, D.K. Robinson, J.M. Blair, A.J. Mallinckrodt, S. McKay, Data reduction and error analysis for the physical sciences, *Comput. Phys.* 7 (1993) 415.
- [58] A. Bondi, van der Waals volumes and radii, *J. Phys. Chem.* 68 (1964) 441.
- [59] J.Y. Park, D.R. Paul, Correlation and prediction of gas permeability in glassy polymer membrane materials via a modified free volume based group contribution method, *J. Memb. Sci.* 125 (1997) 23–39.
- [60] D.W. Van Krevelen, K. Te Nijenhuis, Volumetric properties, in: *Properties of Polymers*, Elsevier, Amsterdam, The Netherlands, 2009, pp. 71–108.
- [61] S. Luo, Q. Zhang, T.K. Bear, T.E. Curtis, R.K. Roeder, C.M. Doherty, A.J. Hill, R. Guo, Triptycene-containing poly(benzoxazole-co-imide) membranes with enhanced mechanical strength for high-performance gas separation, *J. Memb. Sci.* 551 (2018) 305–314.

- [62] C.T. Lee, Development and Advanced Characterization of Novel Chemically Amplified Resists For Next Generation Lithography, Ph.D. Dissertation, Georgia Institute of Technology (2008).
- [63] N.R. Horn, A critical review of free volume and occupied volume calculation methods, *J. Memb. Sci.* 518 (2016) 289–294.
- [64] P.M. Budd, N.B. McKeown, B.S. Ghanem, K.J. Msayib, D. Fritsch, L. Starannikova, N. Belov, O. Sanfirova, Y. Yampolskii, V. Shantarovich, Gas permeation parameters and other physicochemical properties of a polymer of intrinsic microporosity: Polybenzodioxane PIM-1, *J. Memb. Sci.* 325 (2008) 851–860.
- [65] C.L. Staiger, S.J. Pas, A.J. Hill, C.J. Cornelius, Gas separation, free volume distribution, and physical aging of a highly microporous spirobisindane polymer, *Chem. Mater.* 20 (2008) 2606–2608.
- [66] S. Luo, J.R. Wiegand, B. Kazanowska, C.M. Doherty, K. Konstas, A.J. Hill, R. Guo, Finely tuning the free volume architecture in iptycene-containing polyimides for highly selective and fast hydrogen transport, *Macromolecules* 49 (2016) 3395–3405.
- [67] P. Li, T.S. Chung, D.R. Paul, Gas sorption and permeation in PIM-1, *J. Memb. Sci.* 432 (2013) 50–57.
- [68] C.L. Perrin, J.B. Nielson, “Strong” hydrogen bonds in chemistry and biology, *Annu. Rev. Phys. Chem.* 48 (1997) 511–544.
- [69] R. Swaidan, B. Ghanem, E. Litwiller, I. Pinnau, Effects of hydroxyl-functionalization and sub-T_g thermal annealing on high pressure pure- and mixed-gas CO₂/CH₄ separation by

- polyimide membranes based on 6FDA and triptycene-containing dianhydrides, *J. Memb. Sci.* 475 (2015) 571–581.
- [70] A.C. Comer, C.P. Ribeiro, B.D. Freeman, S. Kalakkunnath, D.S. Kalika, Dynamic relaxation characteristics of thermally rearranged aromatic polyimides, *Polymer* 54 (2013) 891–900.
- [71] L.C.E. Struik, Physical aging in amorphous glassy polymers and other materials, *Polym. Eng. Sci.* 17 (1977) 165–173.
- [72] S. Matteucci, Y. Yampolskii, B.D. Freeman, I. Pinnau, Transport of gases and vapors in glassy and rubbery polymers, in: Y. Yampolskii, I. Pinnau, B. D. Freeman (Eds.), *Materials Science of Membranes for Gas and Vapor Separation*, John Wiley & Sons, Chichester, 2006, pp. 1–48.
- [73] X. Jiang, S. He, S. Li, Y. Bai, L. Shao, Penetrating chains mimicking plant root branching to build mechanically robust, ultra-stable CO₂-philic membranes for superior carbon capture, *J. Mater. Chem. A* 7 (2019) 16704–16711.
- [74] M.H. Cohen, D. Turnbull, Molecular transport in liquids and glasses, *J. Chem. Phys.* 31 (1959) 1164–1169.
- [75] S. Japip, G.R. Lee, T.S. Chung, The role of fluorinated aryl ether moiety in polyimide-co-etherimide on gas transport properties, *Ind. Eng. Chem. Res.* 59 (2020) 5315–5323.
- [76] C. Nagel, K. Günther-Schade, D. Fritsch, T. Strunskus, F. Faupel, Free volume and transport properties in highly selective polymer membranes, *Macromolecules* 35 (2002) 2071–2077.

- [77] A. Thran, G. Kroll, F. Faupel, Correlation between fractional free volume and diffusivity of gas molecules in glassy polymers, *J. Polym. Sci. Part B Polym. Phys.* 37 (1999) 3344–3358.
- [78] W.J. Koros, Simplified analysis of gas/polymer selective solubility behavior, *J. Polym. Sci. Polym. Phys. Ed.* 23 (1985) 1611–1628.
- [79] K. Ghosal, R.T. Chern, B.D. Freeman, W.H. Daly, I.I. Negulescu, Effect of basic substituents on gas sorption and permeation in polysulfone, *Macromolecules* 29 (1996) 4360–4369.
- [80] C.R. Mason, L. Maynard-Atem, K.W.J. Heard, B. Satilmis, P.M. Budd, K. Friess, M. Lanci, P. Bernardo, G. Clarizia, J.C. Jansen, Enhancement of CO₂ affinity in a polymer of intrinsic microporosity by amine modification, *Macromolecules* 47 (2014) 1021–1029.
- [81] L.M. Robeson, The upper bound revisited, *J. Memb. Sci.* 320 (2008) 390–400.
- [82] L.M. Robeson, Correlation of separation factor versus permeability for polymeric membranes, *J. Memb. Sci.* 62 (1991) 165–185.
- [83] L.M. Robeson, Z.P. Smith, B.D. Freeman, D.R. Paul, Contributions of diffusion and solubility selectivity to the upper bound analysis for glassy gas separation membranes, *J. Memb. Sci.* 453 (2014) 71–83.

Highlights

- Polymer packing was studied via thermal treatments on functionalized 6FDA-HAB.
- Thermal treatments below the polymer T_g can lead to polymer chain mobility.
- FFV and transport property changes show that extent of treatment affects packing.
- PALS suggests that packing may change from mechanisms besides densification.

Declaration of interests

☒ The authors declare that they have no known competing financial interests or personal relationships that could have appeared to influence the work reported in this paper.

☐ The authors declare the following financial interests/personal relationships which may be considered as potential competing interests: